Available online at www.sciencedirect.com

SciVerse ScienceDirect

journal homepage: www.elsevier.com/locate/he

A WTS power conversion stage with multilevel converters operating in the medium voltage range

*Santiago A. Verne**, *María I. Valla*

Laboratorio de Electrónica Industrial, Control e Instrumentación, Facultad de Ingeniería, Univ. Nac. de La Plata (UNLP) and CONICET, Calle 48 y 116, La Plata, CP 1900, Argentina

ARTICLE INFO

Article history:
Received 26 August 2011
Accepted 13 December 2011
Available online 3 January 2012

Keywords:
Wind energy conversion
Multilevel converters
Model predictive control

ABSTRACT

A high power medium voltage converter for wind turbine system is presented in this paper. The proposal mitigates classic design tradeoffs around low voltage, high current link between the generator and the utility grid on the megawatt range. The power converter is based on Multilevel Converters technology which allows to extend the power-handling capability of the electronic switches, reaching the medium voltage operation without step-up transformers. The converter controllers are based on the Finite-States Model Predictive Control approach, leading to fast dynamic response and *DC* bus voltages equalization. The performance of the control scheme is evaluated with computer simulations.

1. Introduction

Development and evolution of renewable energy systems increases their dependence on power electronic converters. They have gained prominence due to their high control versatility which allows fulfilling both the control requirements stated by the renewable source itself and the grid codes.

In order to increase the energy efficiency, variable-speed operation of modern Wind Turbine Systems (*WTS*) has been widely adopted. Also, the increasing demands of sustainable electric power and a lower cost per megawatt, constantly pushes the boundary of *WTS* to higher power capacity, increasing all sub-systems rating including tower, machinery and power converters. Latest turbines are rated in the range of 3–7.5 MW.

Although modern variable-speed turbines lie on the Doubly Fed Induction Generator (*DFIG*) and field excited Synchronous Generator, the lower prices of strong permanent magnets increased the interest on high power Permanent Magnet Synchronous Generators (*PMSG*) [1]. This machine combines low maintenance with a high power-size ratio and gearless transmission capability, enhancing mechanical efficiency and robustness.

In the megawatt range, the Multilevel Converter (*MC*) is an attractive choice in comparison with the parallel connection of low voltage converters [2]. Multilevel Converter applications such as motor drives, Active Power Filters and FACTS-based Power Quality solutions have been investigated [3]. Particularly, the full-scale Back-to-Back (*B2B*) converter configuration, jointly with *PMSG* allows higher efficiency at the generator side compared with the rectifier–chopper design and also higher controllability. It has major advantages regarding grid code compliance with respect to *DFIG* based solutions, which are limited to approximately 30% of the turbine's rated power. Also, the utilization of Medium Voltage (*MV*) equipment solves problems such as the location of the step-up transformer and the need for the expensive large-

* *Corresponding author*. Tel./fax: +54 (0) 221 425 9306.
E-mail address: santiago.verne@ing.unlp.edu.ar (S.A. Verne).

0360-3199/$ – see front matter
doi:10.1016/j.ijhydene.2011.12.098

diameter cable link between the nacelle and the bottom of the turbine [4]. This suggests that the migration of high power wind generators to medium voltage is unavoidable. Some works deal with this issue, considering various multilevel converter topologies [5]. Multipole Syncronous Generators are also considered [6], and commercial solutions in this area are available at this time.

This work explores the performance of a *B2B* multilevel converter based on the Diode Clamped Multilevel Converter (*DCMC*) which avoids the step-up coupling transformer allowing the direct connection of the *WTS* to the medium voltage grid. Converter control is addressed through Finite-States Model Predictive Control approach (*FS-MPC*), which gives fast dynamic response and it is a natural control strategy to be merged with the *DC* bus voltage balance. The proposal is evaluated through computer simulations.

2. System overview

2.1. System description and control goals

Fig. 1 depicts a block diagram of a *WTS* system comprising a *PMSG* and a Back-to-Back power converter based on the Diode Clamped topology.

The system control goals are the optimization of the wind power resource and a proper interfacing to the utility grid. More precisely, the generator side converter (*GeC*) controls the *PMSG* in order to extract the maximum power from the wind defining the load torque and so the electric power extracted. This power is transferred to the *DC* link, and redirected to the grid at constant frequency by means of the *DC* bus voltage control, which is executed by the grid side converter (*GrC*). Also, when a voltage sag occurs, the *GrC* injects reactive power proportionally to the sag amplitude in order to contribute to the grid voltage restoration.

2.2. Control strategy

The control strategy on both converters is a *FS-MPC* approach which consists on the calculation of target variables from the present sample time k to the next, and their global comparison with the reference values. These variables can be classified as external (line currents or the AC output power) or internal (DC bus capacitors voltages) to the power converters. They are evaluated for each converter switching combination by means of a figure of merit that measures the "distance" between the calculated value and its set point,

$$J = J_{ext} + J_{int} \tag{1}$$

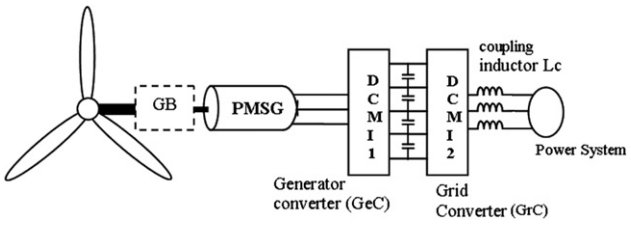

Fig. 1 – WTS block diagram using a five level DCMI.

where, $J_{ext,}$ and J_{int} are the cost functions associated to the external and the internal controlled variables. In the particular case of the Diode Clamped Converter, J_{int} evaluates the balancing state of the DC bus in order to maintain all capacitors voltages at the same value. This is achieved through the function (2):

$$J_{int} = J_V = \frac{1}{4}\sum_{i=1}^{4}\frac{\left|V_{Cref} - V_{Ci}[k+1]\right|}{V_{Cref}} \tag{2}$$

which evaluates the average voltage error (with respect to the reference values V_{Cref}) on capacitors voltages due to the three line currents for all the switching combinations [7]. This term is common to both converters.

The generator converter is controlled with a Predictive Current Control. It optimizes the working point of the *PMSG*, through torque and reactive current control by means of the cost function g_{ext}, while voltage balance control is addressed through the term g_{int} according to:

$$g_{GeC} = g_{ext} + g_{int} = \left(K_{i_q} g_{i_q} + K_{i_d} g_{i_d}\right) + \left(K_{VGeC} J_V\right) \tag{3}$$

where g_{i_q} and g_{i_d} are the cost functions related to the generator synchronous currents (external variables) and J_V evaluates the *DC* bus voltage balance (internal variables), and K_i are their respective weighting factors, which allow to emphasize the importance of each component in the optimization process.

The *GrC* uses a Predictive Power Control. It stabilizes the *DC* bus voltage by regulating the power transferred to the grid. It also controls the reactive power to comply with the grid code policy in case of a fault or to set the power factor to unity in normal operation. The same as the *GeC*, the *GrC* controller takes care of the voltage balance, leading to the cost function,

$$h_{GrC} = h_{ext} + h_{int} = \left(K_P h_P + K_Q h_Q\right) + \left(K_{VGrC} J_V\right) \tag{4}$$

Here, h_P and h_Q are the cost functions associated with active and reactive power injected to the grid (external variables), and J_V has the same meaning as before.

3. Generator converter control

The goal for the *GeC* is to maximize the power extracted from the turbine. This is accomplished by exerting an adequate load torque on the generator so that the tip-speed ratio λ remains at its optimal value λ_{opt}. This depends on the wind speed V_W:

$$\lambda_{opt} = \frac{\omega_{opt} R}{V_W} \tag{5}$$

When this condition is present, the maximum power that can be extracted, and the corresponding torque are:

$$P_{max} = \frac{1}{2}\rho\pi R^2 V_W^3 C_{Pmax},\ T_{opt} = \frac{1}{2}\rho\pi R^3 \frac{C_{Pmax}}{\lambda_{opt}^3}\omega_{opt}^2 \tag{6}$$

where ρ is the air density, R the turbine radius and C_{Pmax} the power coefficient at $\lambda = \lambda_{opt}$. The generator converter is devoted to control the line currents in order to adjust the torque at its optimal value. This is achieved by means of proper selection of *GeC* output voltages. The phase voltage on the motor windings is calculated in terms of converter line voltages through (7):

$$V = \begin{bmatrix} V_a \\ V_b \\ V_c \end{bmatrix} = \frac{1}{3}\begin{bmatrix} 2 & 1 \\ -1 & 1 \\ -1 & -2 \end{bmatrix}\begin{bmatrix} V_{ab} \\ V_{bc} \end{bmatrix} \quad (7)$$

The *PMSG* dynamic equation is (Fig. 2):

$$\mathbf{V} = R_s\mathbf{i} + \frac{d\psi_s}{dt} \quad \text{with } \psi_s = L_s\mathbf{i} + \psi_m e^{j\theta_r} \quad (8)$$

where $\mathbf{i}$ is the line current and ψ_s the flux linking the stator windings that depends on the flux produced by the rotor magnets (ψ_m) and the stator current. Transforming to the $d-q$ rotor reference frame yields to the electrical equation (9), where P represents the number of pole pairs of the generator:

$$\frac{di_d}{dt} = \frac{1}{L_d}V_d - \frac{R}{L_d}i_d + \frac{L_q}{L_d}P\omega_r i_q \quad (9a)$$

$$\frac{di_q}{dt} = \frac{1}{L_q}V_q - \frac{R_s}{L_q}i_q - \frac{L_d}{L_q}P\omega_r i_d - \frac{\psi_m P\omega_r}{L_q} \quad (9b)$$

Performing a forward Euler approximation on (9a) and (9b) gives:

$$\begin{aligned} i_d[k+1] &= T_S\left(\frac{1}{L_d}V_d[k] - \frac{R_s}{L_d}i_d[k] + \frac{L_q}{L_d}P\omega_r i_q[k]\right) + i_d[k] \\ i_q[k+1] &= T_S\left(\frac{1}{L_q}V_q[k] - \frac{R_s}{L_q}i_q[k] - \frac{L_d}{L_q}P\omega_r i_d[k] - \frac{\psi_m P\omega_r}{L_q}\right) + i_q[k] \end{aligned} \quad (10)$$

Equation (10) expresses the current components at instant $k+1$ as a function of system parameters, their values at instant k and converter's voltage.

At every instant, the corresponding current references i_q^* and i_d^* must be tracked, as they are related to the reactive current component and the generator load torque, respectively. Given that unity power factor is desired, a zero reference is defined for i_d^* and the active component is defined through the machine mechanical equation. This is resumed in (11):

$$i_q^*[k] = \frac{2}{3P\psi_m}\frac{T_{opt}[k]}{K_{gearbox}}, \; i_d^* = 0 \quad (11)$$

As the power converter has a discrete number of switching combinations, each one of them is introduced in equation (10) giving a set of values of i_d and i_q. To select the most adequate switching combination, cost functions that measure the "distance" between the reference values and the predicted has the expression (12) for both current components:

$$g_{i_d} = \frac{\left|i_d[k+1] - i_d^*\right|}{i_{rated}} \quad g_{i_q} = \frac{\left|i_q[k+1] - i_q^*[k]\right|}{i_{rated}} \quad (12)$$

Then, the optimization of machine variables can be realized through a joint optimization function that takes both components as:

$$g_{ext} = K_{i_q}g_{i_q} + K_{i_d}g_{i_d} \quad (13)$$

Fig. 2 shows a block diagram of the control scheme.

4. Grid converter control

The high penetration of alternative energy systems has motivated regulations with respect to the connection holding time when a fault occurs and also ancillary services like reactive power injection [8]. A grid code profile describes the disconnection boundary as a function of time depending on the voltage sag magnitude and its duration and also the amount of reactive current, relative to the system's rated current, depending on the sag amplitude. Whether the reactive power is injected to the grid, active power transfer should be reduced or even canceled to avoid exceeding the rated current of the *GrC*. Then, during the fault, the generator must be de-loaded to avoid the excessive increase of the *DC* bus

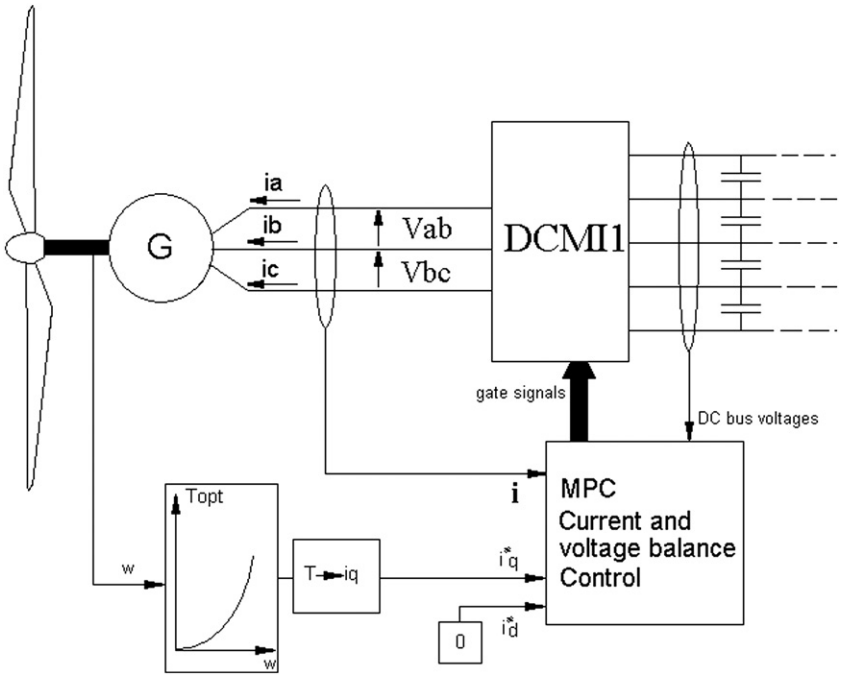

Fig. 2 – Generator side converter control diagram.

voltage. Although this causes the turbine acceleration, the high value of the rotor inertia causes small speed increase in its rotational speed. In addition, if the fault exceeds the time of connection holding, the pitch angle control (which is not considered in this study) can prevent from over speed.

4.1. Active and reactive power calculation

The predictive strategy lies on the calculation of real and imaginary power for all the switching combinations [9]. For this, future value of line currents are calculated with reference to Fig. 3. At a given sampling instant k, phase voltages $\mathbf{e}[k]$ and currents $\mathbf{i}[k]$ are sampled. The active and reactive power supplied by the AC system at instant $(k+1)$ can be calculated applying the Instantaneous Power Theory, through a prediction of the line currents. This calculation is performed evaluating (14) where it is suposed that the system voltage $\boldsymbol{e}$ remains constant during T_S ($\mathbf{e}[k+1] \approx \mathbf{e}[k]$).

$$\begin{bmatrix} i_a \\ i_b \\ i_c \end{bmatrix}_{K+1} = \frac{T_S}{3L_C}\left(\begin{bmatrix} -2 & -1 \\ 1 & -1 \\ 1 & 2 \end{bmatrix}\left(\begin{bmatrix} V_{ab} \\ V_{bc} \end{bmatrix}_K - \begin{bmatrix} e_{ab} \\ e_{bc} \end{bmatrix}_K\right)\right) + \left(1 - \frac{r_C T_S}{L_C}\right)\begin{bmatrix} i_a \\ i_b \\ i_c \end{bmatrix}\Bigg|_K \tag{14}$$

where T_S is the sampling period, r_c the coupling inductor resistance and e_{xy}, V_{xy} the line voltages at the power system and the converter sides, respectively. Using the stationary transformation, active and reactive power supplied by the AC system can be calculated with expression (15).

$$\begin{aligned} P[k+1] &= e_\alpha[k] i_\alpha[k+1] + e_\beta[k] i_\beta[k+1] \\ Q[k+1] &= e_\beta[k] i_\alpha[k+1] - e_\alpha[k] i_\beta[k+1] \end{aligned} \tag{15}$$

The optimization functions associated with P and Q are designed to track these variables to their reference values. Individual cost functions are defined in (16) for P and Q, normalized to the rated power of the converter:

$$h_P = \frac{|P[k+1] - P^*[k+1]|}{P_{rated}} \quad h_Q = \frac{|Q[k+1] - Q^*[k+1]|}{P_{rated}} \tag{16}$$

and the power optimization is given by (17):

$$h_{ext} = K_P h_P + K_P h_Q \tag{17}$$

The reference value Q* of reactive power is set depending on the power mode as described before (normal or fault mode). The active power reference P* is shaped summing up the consumed power on the inverter side and the necessary power to regulate the DC bus voltage [10]. On the other hand, the reactive power reference Q* is set depending on the operation mode of the GrC. If the grid voltage is within the 10% band, it is set to zero, and if fault mode is present, it is set to a value that depends on the grid code.

In normal operation, the control target of the GrC is the DC link voltage regulation. Also, in normal grid conditions a high power factor presented to the utility grid is desired. The same as the generator converter, the control algorithm also takes

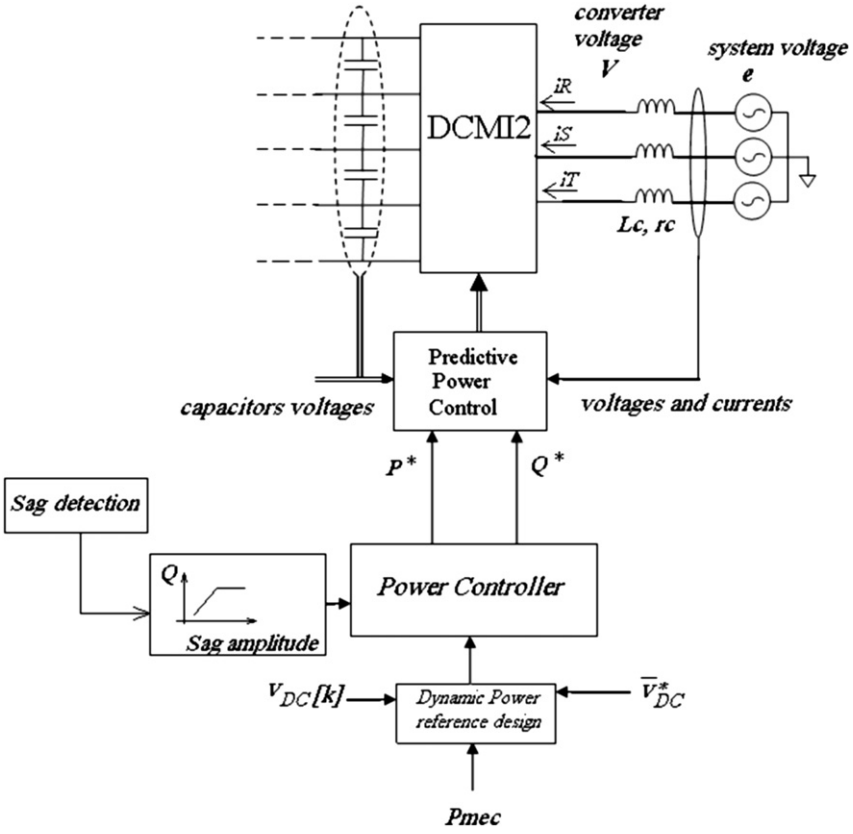

Fig. 3 – Grid side converter control diagram.

into account the capacitors balancing issue by selecting the best switching combinations in order to minimize the cost function.

5. Performance evaluation

The proposed control strategy is evaluated for a 3 MW wind turbine with computer simulations. The system performance is evaluated in both normal and fault mode conditions of the AC grid, in order to analyze the behavior of the electrical and mechanical variables. The *DC* bus is rated 20 kV for direct connection to the medium voltage grid, with 1500 μF–5 kV DC capacitors and a grid coupling inductor *Lc* =10 mH. The sampling frequency is set to 6 kHz, and the total moment of inertia is considered $J = 10^6$ kgm^2.

The first test shows the results of system variables for two values of wind speed. At $t = 0$, the turbine rotates at a speed close to 15 *RPM* for a wind speed $V_W = 10$ m/s (Fig. 4(a)), delivering an active power of approximately 1.9 MW. In $t = 0.3$ s, wind value is increased to $V_W = 11.8$ m/s, which is considered the rated value. The turbine's rotor speed increases up to 17.5RPM, reaching a power output of 2.9 MW. As it can be seen, the rotor speed takes about 14 s to converge to the final value. The resistant torque (Fig. 4(b)) also increases reaching a maximum value of 150 kNm. Fig. 5 depicts currents and voltages of the *GrC* and *GeC*, respectively for both wind speed values. It can be seen the corresponding phase shift between line voltage and currents which is near 30°. For better visualization, the currents are amplified by factor of 50. Fig. 5(a) shows the *GrC* line voltage and current, while Fig. 5(b) shows the same variables for the *GeC* for the reduced wind speed regime ($V_W = 10$ m/s, $0 < t < 0.3$ s). The line voltage presents the typical staircase waveform of the multilevel converters, while highly sinusoidal current is achieved. It is observed in this case that the *GeC* voltage uses a reduced number of voltage levels due to the lower-than-rated speed of the PMSG and consequently the *EMF*. Fig. 5(c) and (d) ($t >> 0.2$ s) show the same set of variables as before. While the *GrC* uses the same voltage levels as the previous case (the grid peak voltage remains unchanged), the *GeC* uses more levels as the speed and consequently the *EMF* of the generator has increased. Also

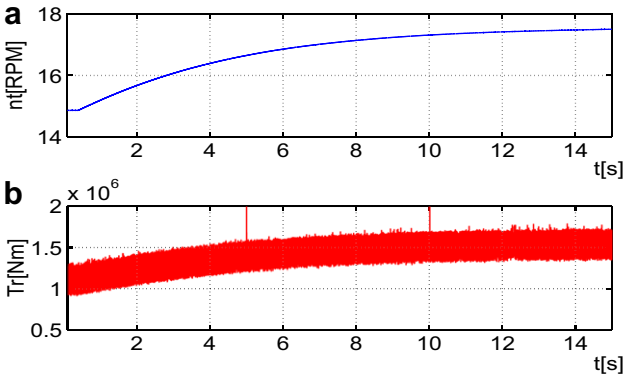

Fig. 4 – (a) Turbine Speed (b) Resistant torque.

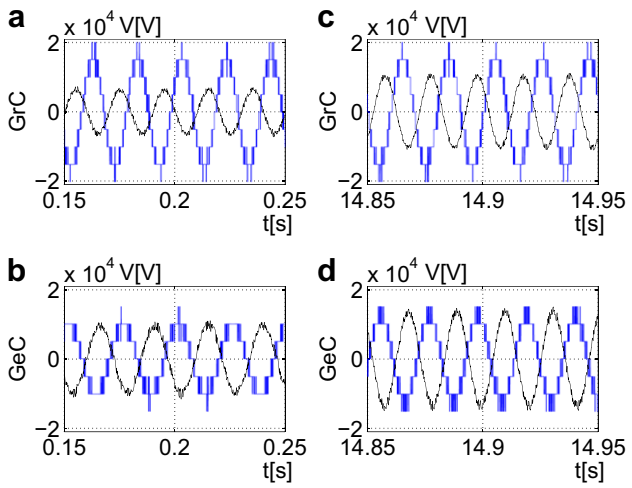

Fig. 5 – Currents and voltages on *GrC* and *GeC* for two wind speeds, (a),(b) $V_W = 10$ m/s, (c),(d) $V_W = 11.8$ m/s.

both current increase, in order to reach the system output power to approximately 2.9 MW.

The second test shows the effect of a grid voltage sag and the reactive current injection required by the grid code for voltage restoration. The operation is set with a wind speed (10.8 m/s) and an output power of 2 MW. At $t = 0.2$ s, a 30% voltage sag is introduced.

According to the grid code, 60% of the converter's rated current must be injected with reactive power factor in order to contribute to the grid voltage restoration. The conversion system should be able to handle this condition for at least 2.2 s and resume at normal condition after the fault. Fig. 6 shows the corresponding voltages and currents at both converters *AC* terminals. Fig. 6(a) shows a *GrC* line voltage and current around the fault region, while Fig. 6(b) shows the line voltage and current at the *GeC* terminals. The converter voltage levels usage during the sag is reduced in order to

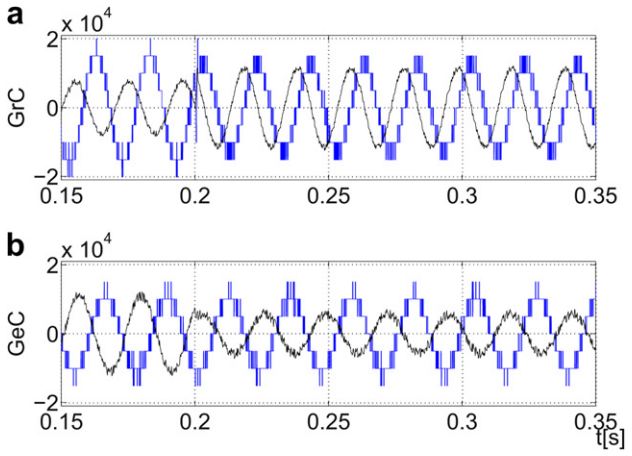

Fig. 6 – Converter Voltage and currents for rated wind speed (a) *GrC* voltage and current, (b) *GeC* voltage and current.

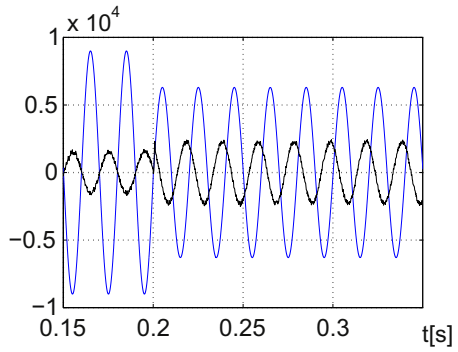

Fig. 7 – Grid phase voltage and its corresponding current.

reach the desired reactive current value. In Fig. 6(b), the partial generator de-loading is observed through the reduction of the current drawn from the machine. Fig. 7 shows one grid phase voltage and the corresponding current, during this event. It can be observed that the required current phase shift for grid code fulfillment is rapidly reached from pure active to partially active and reactive. This ratio is determined by the reactive demand from the grid code and from the remaining current capacity that is assigned to the active current component.

The mechanical variables of the generator are shown in Fig. 8 including the fault. The *EM* torque is shown in 8(c) and the turbine speed in 8(a). Acceleration is observed within the sag occurrence, which is not significant due to the high value of rotor inertia and the partial braking due to residual active power transfer. Turbine speed is 16RPM and raises 17RPM at the end of the fault. Then, the rotational energy in excess of the mechanical system is evacuated after the grid restoration reaching 2.5 MW at $t = 2.3$ s. The active and reactive power are measured at the grid side and are also shown in Fig. 8. It is observed that within the fault time, the active power transfer is reduced from 2 MW to 1.2 MW due to generator partial de-loading when the fault occurs (Fig. 8(b)).

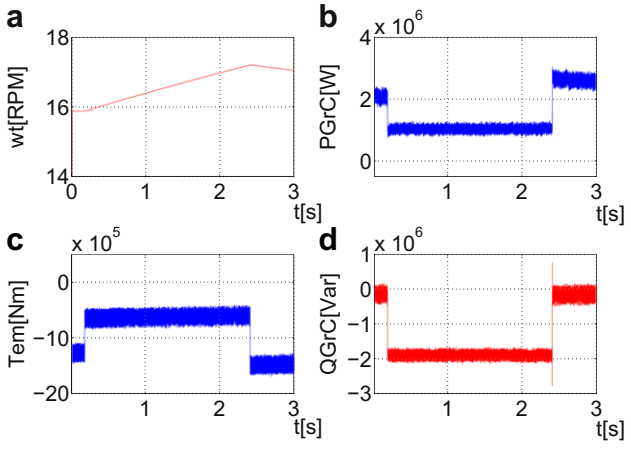

Fig. 8 – (a) Turbine speed, (b) Power injected to the grid by *GrC*, (c) Resistant torque, (d) Reactive Power consumed from the grid.

Fast dynamic response on reactive power injection is observed in Fig. 8(d) which tends to counteract the grid voltage level.

6. Conclusions

A transformerless multilevel power electronic converter for a *WTS* was presented. It has been demonstrated that the *B2B* power interface has good performance regarding the main control objectives and also presents reliable potential to fulfill ancillary services required by the grid operator. A satisfactory evaluation can be made with respect to the control of power converters and their internal variables by means of the Finite-States Model Predictive Control strategy.

Acknowledgments

This work was supported by Univ, Nac. de La Plata (UNLP), CONICET and ANPCyT.

REFERENCES

[1] Chen Z, Guerrero J, Blaajberg F. A review of the state of the art of power electronics for wind turbines. IEEE Trans Power Electron 2009;24:1859–75.
[2] Kouro S, Malinowski M, Gopakumar K, Pou J, Franquelo LG, Wu B, et al. Recent advances and industrial applications of multilevel converters. IEEE Trans Ind Electron 2010;57:2553–80.
[3] Abu-Rub H, Holtz J, Rodriguez J, Baoming G. Medium voltage multilevel converters – state of the art, challenges, and requirements in industrial applications. IEEE Trans Ind Electron 2010;57:2581–95.
[4] Ng Chong H, Parker MA, Ran L, Tavner PJ, Bumby JR, Spooner E. A multilevel modular converter for a large, light weight wind turbine generator. IEEE Trans. Power Electron 2008;23:1062–74.
[5] Melício R, Mendes VMF, Catalão JPS. Power converter topologies for wind energy conversion systems: integrated modelling, control strategy and performance simulation. Renew Energy 2010;35:2165–74.
[6] Abbes M, Belhadj J, Bennani ABA. Design and control of a direct drive wind turbine equipped with multilevel converters. Ren Energy 2010;35:936–45.
[7] Verne SA, González SA, Valla MI. An optimization algorithm for capacitor voltage balance of N-level diode clamped inverters, 34th Annual Int. Conf. of the IEEE Industrial Electronics Soc (IECON'08), Orlando, FL, USA, 2008. p. 3201–3206.
[8] Alepuz S, Busquets-Monge S, Bordonau J, Cortés P, Kouro S. Control methods for low voltage ride-through compliance in grid-connected NPC converter based wind power systems using predictive control. In: Energy conversion congress and exposition (ECCE 2009); 2009. p. 363–9.
[9] Verne SA, Valla MI. Active power filter for medium voltage networks with predictive current control. Electr Power Syst Res 2010;80(12):1543–51.
[10] Quevedo DE, Aguilera RP, Pérez MA, Cortés P. 2010 Finite control set MPC of an AFE rectifier with dynamic references. Intl. Conf. on Ind. Techn. (ICIT2010), p. 1265–70.